Monte Carlo simulation of solute aggregation in binary alloys: Domain boundary precipitation and domain growth

J.-M. Liu*
Laboratory of Solid State Microstructures, Nanjing University, Nanjing 210093, China
and Institute of Materials Research & Engineering, Lower Kent Ridge Road, Singapore 119260

L. C. Lim
Department of Mechanical and Production Engineering, National University of Singapore, Singapore 119260

Z. G. Liu
Laboratory of Solid State Microstructures, Nanjing University, Nanjing 210093, China
(Received 27 July 1998; revised manuscript received 17 February 1999)

Domain boundary precipitation and domain growth in binary polycrystalline materials are studied by applying the Monte Carlo simulation in two-dimensional squared lattice. The simulation is carried out on a hybrid lattice of the kinetic spin-exchange Ising model coupled with the Q-state Potts model. First of all, the static properties of this coupled model are studied, predicting just a small shiftdown of the critical point with enhanced Potts interactions. Subsequently, the dynamic properties, such as morphology and coarsening kinetics of the second phase precipitates as well as kinetics and scaling of the domain growth, are investigated in detail. Pronounced second phase precipitation at domain boundaries is observed at a temperature range just below critical point T_c as long as the solutes prefer to segregate onto the boundaries. However, the boundary precipitation is significantly prohibited at either high or low temperatures ($T \gg T_c$ or $T \ll T_c$). We demonstrate that the domain growth is slowed down due to the pinning effect of the precipitates at the boundaries, no matter what the boundary migration ability is. The kinetics of boundary precipitation and domain growth in various systems are simulated. Both the Lifshitz-Slyozov-Wagner law for second phase coarsening and the linear law for the normal domain growth become broken due to the domain boundary precipitation. The scaling behavior of the domain growth is identified in present systems although a further confirmation may be required. [S0163-1829(99)00434-8]

I. INTRODUCTION

When a solid solution is submitted into the two-phase coexisting range of the temperature-composition diagram, a second phase precipitates from the matrix of the parent phase. This problem represents one of the fundamental fields in condensed matters and materials science. For a homogeneous system, the early stage of precipitation may be identified as either nucleation, consequent growth and coarsening of the second phase, or spinodal decomposition, depending on temperature T and alloy composition C_0.[1–4] Much effort in development of microscopic techniques has been made in last decade in order to study the very early stage of precipitation, although the short time and nanospatial scales make it a big challenge to the researchers.[1,3] Up to date, the theoretical scheme of phase precipitation may not be so optimistic, there still remain some uncertainties due to the great complexity of the problem.[1,3,4] Nevertheless, toward the late stage the physical picture becomes simple. The two-phase microstructure can be characterized with the spatial correlation function $g(r,t)$, which exhibits unique characteristic length and follows the scaling concept.[5–7] The characteristic length l_c evolves according to the well-known Lifshitz-Slyozov-Wagner (LSW) law.[8,9] This law has recently been demonstrated even for the highly concentrated alloys as long as the system is of short-range interaction, noting that several other laws were proposed previously.[10–12]

The real materials may not be always homogeneous, where various types of defects like vacancies, dislocations, domain boundaries (DB's) and so on, are involved. The preferable precipitation of the second phase around these defects was observed a long time ago.[13] In particular, vacancies are helpful for phase precipitation. Due to structural difference, the new phase may introduce elastic strain, which modulates the morphology and changes the kinetics of precipitation.[14] In this case, controversial results on the late stage kinetics of precipitation were reported.[10–12,15] Furthermore, most materials under service are polycrystalline so that the domain (grain) boundaries must be considered.[13] In fact, the materials' property depends essentially on domain size, while domain boundary segregation is a common phenomenon in materials processing.[16–21] This allows one to argue that the real kinetics of second phase precipitation may be very different from the homogeneous phase transformations.

On the other hand, domain growth represents a common materials process. Growth of the larger domains in concert with shrinking of the smaller ones is driven by the excess free energy associated with the DB's.[22,23] For two-dimensional lattice, it is well understood that apart from the very early stage, the average domain size follows the well-known kinetics of $\langle A \rangle \sim t$, where $\langle A \rangle$ is the average domain area and t is time. The normalized domain size distribution keeps stationary with time, i.e., the so-called scaling

state.[24–26] However, a new complexity appears as the domain growth is coupled with additional processes, for example, when domain boundary segregation or precipitation occurs in parallel.[17] The domain growth is then expected to be pinned by segregated solutes or precipitates at DB's. The boundary property will be significantly modified too. These problems have been of special interest to physicists and materials researchers. For example, Fan and co-workers[27,28] investigated the diffusion controlled domain growth with second phase precipitates trapped at DB's. A series of new effects are predicted from their phase-field theory that is critical to our understanding of the coupling phenomena during microstructural evolution of multiphased materials.

In a previous paper[29] we developed a Monte Carlo (MC) approach of a hybrid model in which the kinetic spin-exchange Ising model[30,31] and the Q-state Potts model[32] are combined in order to study the solute segregation phenomenon at DB's. The domain boundary segregation in binary multidomained alloys was simulated in detail. This approach can be directly extended to simulate phase precipitation problems in such a system. Furthermore, a study of the static properties of such a hybrid model is essential too. In particular, the critical point T_c of the system where highly degenerated states (Potts spins) are introduced may be different from the pure Ising system conventionally applied to approach phase precipitation. In this article, we are going to study by the MC method the static properties of this hybrid system. Then, a detailed simulation of the second phase precipitation in this system will be done, whereas domain growth is considered as a parallel sequence. We pay attention to the kinetics of domain boundary precipitation and domain growth. The problems we are interested in are: dependence of T_c on the Potts-spin interaction, morphology and kinetic features of the precipitates at DB's, the LSW law to be confirmed in this hybrid model, dynamic scaling behavior, domain growth kinetics, and scaling of domain size distribution. After main results are presented, some relevance of our model with real alloy systems will be discussed, such as the effect of vacancies and ordered compound precipitates. The remaining part of this paper is organized as follow. In Sec. II we will briefly describe the hybrid mode. The static properties of this model will be studied in Sec. III and the simulated results of the kinetics will be presented in Sec. IV with extended discussion. In Sec. V we explore the possible relevance of this model with real alloy systems. The conclusion will be given in Sec. VI.

II. BRIEF DESCRIPTION OF MODEL

In our approach we assume that the phase transformation is diffusion dominant, without involving lattice reconstruction. The approach is developed for the two-dimensional case. An extension to the three-dimensional one is direct.

We start from a two-dimensional squared $L\times L$ lattice with periodic boundary conditions applied. For modeling species diffusion in the lattice, the spin-exchange Ising model is used, with conserved number of total spin states.[30,31] Each site is occupied by one species, A or B, with the Ising spin parameter $S_i=0$ for A and $S_i=1$ for B. The alloy composition is then $C_0=N_B/(N_A+N_B)$, where N_A and N_B are the numbers of species A and B, respectively, and the total spin number $N=N_A+N_B$. In our model, only the nearest-neighboring part of the spin-interaction is accounted for. What we should point out here is that the diffusion in real alloys performs via the spin-vacancy exchange[33] instead of the direct spin-exchange mechanism assumed here. We shall come back to this argument in Sec. V A. On the other hand, the domain degeneracy of the lattice is expressed by Q spins in the Q-state Potts model and upon each site is imposed one of the Q multispin states. The Potts spin of a site represents its lattice orientation. A closed lattice area of identical spin represents one domain. If two nearest-neighboring sites have different spin states, it means that they are on the DB's. The high-energy state of domain boundary sites acts as the driving force for boundary migration and then domain growth. We assume that the Ising interaction between two neighboring sites has nothing to do with their Potts spins, whether they are identical or different. This means that the Ising interaction between two nearest-neighboring sites is independent of their location, either on DB's or inside one domain. The Hamiltonian of the present system, H, can be written as follows, a detailed derivation of which refers to our previous paper:[29]

$$\begin{aligned}
H&=H_I+H_P\\
&=-\Bigg[\phi_{AA}\sum_{\langle ij\rangle}(1-S_i)(1-S_j)+\phi_{BB}\sum_{\langle ij\rangle}S_iS_j\\
&\quad+\phi_{AB}\sum_{\langle ij\rangle}S_i(1-S_j)+(1-S_i)S_j\Bigg]\\
&\quad-J_{AA}\sum_{\langle ij\rangle}(1-S_i)(1-S_j)[(1-f_{AA})+f_{AA}\delta_{\mathrm{Kr}}(\alpha,\beta)]\\
&\quad-J_{BB}\sum_{\langle ij\rangle}S_iS_j[(1-f_{BB})+f_{BB}\delta_{\mathrm{Kr}}(\alpha,\beta)]\\
&\quad-J_{AB}\sum_{\langle ij\rangle}[S_i(1-S_j)+(1-S_i)S_j]\\
&\quad\times[(1-f_{AB})+f_{AB}\delta_{\mathrm{Kr}}(\alpha,\beta)],
\end{aligned}\tag{1}$$

where H_I and H_P represent the Ising part and Potts part of H, respectively; ϕ_{mn} $(m,n=A,B)$ denotes the Ising interaction of nearest-neighboring m-n pair; $\langle ij\rangle$ represents that over nearest neighbors is summed once; J_{mn} $(\geqslant 0)$ is the Potts interaction factor associated with the Potts-spin pair between the Ising spins m and n; δ_{Kr} is the Kronecker δ function which is defined as[32]

$$\delta_{\mathrm{Kr}}=\lfloor 1+(Q-1)\vec{e}^{\,\alpha}\cdot\vec{e}^{\,\beta}\rfloor/Q,\tag{2a}$$

where $\vec{e}^{\,\alpha}$ $(\alpha=1,2,\ldots,Q)$ are Q unit vectors pointing in the Q symmetric directions of a hypertetrahedron in $Q-1$ dimensions. However, this formula can be simplified in two-dimensional lattice, i.e., the planar Potts model is utilized instead of the standard Potts model:[32]

$$\delta_{\mathrm{Kr}}=\cos\left(2\pi\frac{\alpha-\beta}{Q}\right).\tag{2b}$$

In Eq. (1) an important variable which defines the behavior of domain boundary segregation is f_{mn} $(m,n=A,B)$ (0

$\leqslant f_{mn} \leqslant 1$), a factor to scale the Potts interaction between Ising spins m-n. As an example for better understanding of factor f_{mn}, one writes the Potts interaction for Ising spin-pair B-B as

$$H_P^{BB} = -J_{BB} \sum_{\langle ij \rangle} S_i S_j [(1-f_{BB}) + f_{BB} \delta_{\mathrm{Kr}}(\alpha,\beta)], \quad (3a)$$

where $S_i = S_j = 1$. One obtains two extreme situations:

$$H_P^{BB} = \begin{cases} -J_{BB} \cdot C_0 \cdot L^2, & \text{minimal as } f_{BB} = 0 \\ -J_{BB} \sum_{\langle ij \rangle} S_i S_j \delta_{\mathrm{Kr}}(\alpha,\beta), & \text{maximal as } f_{BB} = 1. \end{cases} \quad (3b)$$

At $f_{BB} = 0$, H_P^{BB} takes the minimal energy state, showing no (α,β) dependence. The dynamic relaxation of the system will drive B-B pairs toward the DB's whose excess boundary energy can then be dissipated. Therefore segregation of B-B pairs onto those DB's becomes thermodynamically favorable and irreversible. However, no favorable tendency of B-B pair segregation can be seen if $f_{BB} = 1.0$, because H_P^{BB} is completely (α,β) dependent. It reaches the maximum as a function of f_{BB}. As $0 < f_{BB} < 1$, the boundary segregation of B-B pairs is still favorable but less serious than the case of $f_{BB} = 0$. The same behavior is observed, referred to as either A-A pair or A-B pair. For the reason of simplification, $f_{AB} = (f_{AA} + f_{BB})/2$ is always taken in our approach, whatever f_{AA} or f_{BB} takes.

As $\phi_{mm} = 0$ and $\phi_{AB} < 0$, it is seen that there is no interaction between the like Ising pair but repulsive force between the unlike pair, respectively. This results in phase aggregation of the like Ising spins, i.e., second phase precipitation.[34] In fact, $\phi_{mm} = 0$ is not the necessary condition for phase precipitation. Here we define an effective interaction factor $\phi = (\phi_{AA} + \phi_{BB})/2 - \phi_{AB}$, so T/T_c, where $kT_c/\phi = 1.13 \sim 1.00$ and k is the Boltzmann constant represents the normalized temperature of the system with respect to T_c. In our lattice, there is no probability to form ordered second phase if only the nearest-neighboring interaction is taken into account.[3,35,36] Our simulation is restricted to the conventional regular solid solutions where there is no involvement of disorder-order transition during precipitation. This restriction may be released to some extent that ordered second phase is observable when the next-nearest-neighboring interaction is considered. We will come back this point in Sec. V.

III. STATIC PROPERTIES OF COUPLING MODEL

In this part we study the static property of the lattice, referring to the Ising spin interaction coupled with the Potts spins, as defined in Eq. (1). In more detail, we study dependence of the Ising criticality on the Potts-spin interaction (J_{mn}, f_{mn}, and domain size R). We want to ensure that the dependence, if any, is not prominent, so that a conventional MC approach of the Ising spin exchange for phase precipitation can be employed. As well reported previously, it is more convenient to deal with the static property in a grand-canonical ensemble.[34] There the chemical potential difference $\mu_A - \mu_B$ is kept constant whiles $C_0 = N_B/(N_A + N_B)$ is permitted to fluctuate, so that any evolution of the structural ordering parameter can be identified. This is different from the case in real alloys, where C_0 remains fixed.

It is obvious that the hybrid model Eq. (1) still shows pairwise interaction as long as f_{mn} $(m,n = A,B)$ remain identical to each other. Therefore phase coexistence and Ising criticality appear at $\mu_A = \mu_B$, predicting that the critical point is located at $C_0 = 0.5$. However, if one deals with domain boundary segregation where $f_{BB} \neq f_{AA}$, the critical point may shift a little from $C_0 = 0.5$. Even so, a subcritical behavior at $C_0 = 0.5$ is still helpful for our understanding of the problem. Our simulation is made around $C_0 = 0.5$. The MC procedure was proposed previously,[34] a brief outline of which is given below.

For given system parameters, an initial lattice configuration is chosen where the Ising spin for each site is imposed at random, satisfying $C_0 = \text{constant}$. A multidomain configuration is folded onto the lattice by randomly imposing a series of circlelike domains until all lattice sites are occupied with Potts spins. The later-deposited domains may overlap the earlier ones, resulting in a distribution of the domain size over a range centered at R. This initial lattice configuration may be constructed via other ways, such as depositing triangle, square or hexagon domains, however, the dynamic feature shows no substantial difference. On simulation, the lattice sites are chosen one by one in regular fashion. When a site is taken by A (or B), it is considered a replacement by B (or A), respectively. However, such a replacement follows a transition probability:

$$W = \exp(-\Delta H/kT), \quad (4)$$

where ΔH is the energy change of such a replacement, calculated according to Eq. (1). If $W < 1.0$, a random number R' uniformly distributed between zero and one will be generated and compared with W. The replacement will be approved as $R' < W$ and refused otherwise. This process is continued until a given set of simulation circles is reached.

The order parameter ψ of the transition is defined as[37]

$$\psi = \frac{1}{L^2} \sum_{\langle j \rangle} (1 - 2S_i), \qquad U_L = 1 - \frac{\langle \psi^4 \rangle_T}{3 \langle \psi^2 \rangle_T^2}, \quad (5)$$

where U_L is the reduced fourth-order cumulant of the order parameter. It has the following properties:

TABLE I. System parameters for static property simulation.

C_0	ϕ_{AA}	ϕ_{BB}	kT/ϕ	J_{mn}/ϕ $(m,n = A,B)$	L	R	f_{AA}	f_{BB}
0.50	0.00	0.00	0.85–1.20	0.0–1.20	32–128	10	1.0	0.0 or 1.0

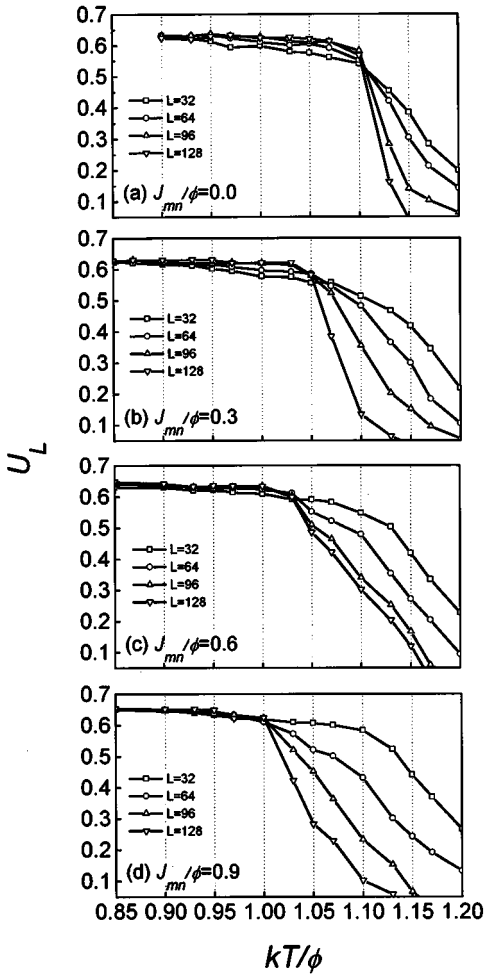

FIG. 1. Fourth-order cumulant U_L as a function of kT/ϕ at various lattice size L for systems of different Potts interaction J_{mn}.

$$\begin{cases} U_L \to 2/3 \text{ as } L\to\infty & \text{for } T<T_c \\ U_L \approx 0.62 & \text{at } T=T_c \\ U_L \to 0 \text{ as } L\to\infty & \text{for } T>T_c \end{cases} . \tag{6}$$

Basically, the position of T_c is determined by evaluating the simulated U_L from lattices of various dimension L and finding their intersection position, as being plotted as a function of temperature T scaled by factor ϕ, because U_L is independent of L at T_c.

The system parameters as chosen are listed in Table I. We study the dependence of T_c on three parameters, J_{mn}, f_{mn} $(m,n=A,B)$, and R, as defined in the Potts model. Note that $R=10$ is chosen here because L starting from 32 is taken and $L \gg R$ should be satisfied. Figure 1 shows the simulated results at $f_{AA}=f_{BB}=1.0$ where the cumulant U_L is plotted against kT at various J_{mn}. Both kT and J_{mn} are scaled with ϕ. At each case, U_L grows gradually with decreasing temperature until a saturated value at low kT. For a fixed J_{mn}, $U_L \sim kT$ curves for the four values of L roughly show a common intersection point $(kT_c, U_L(T_c))$. Note that $U_L(T_c)$ deviates not far from 0.62 and the saturated value of U_L is close to $\frac{2}{3}$ too. It is seen that the critical point T_c shifts a little downward with increasing J_{mn}. At $J_{mn}=0$, $kT_c/\phi=1.12$, quite close to 1.13, the critical point of the Ising model. As $J_{mn}/\phi=0.90$, kT_c/ϕ shifts to 1.02, not so much lower than the value at $J_{mn}=0$. It is then demonstrated that T_c is not so much sensitive to J_{mn}.

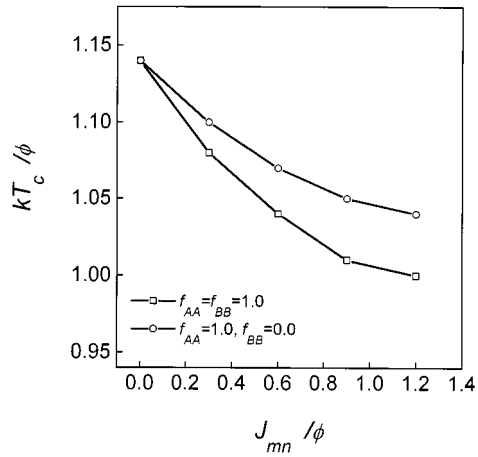

FIG. 2. Critical point T_c vs the Potts interaction factor J_{mn} at various values of f_{mn}.

As $f_{AA}=1.0$ but $f_{BB}=0.0$, a downward shift of T_c with increasing J_{mn} is still observable. However, the shift is less than the case of $f_{AA}=f_{BB}=1.0$. The simulated data are given in Fig. 2, where kT_c/ϕ is plotted vs J_{mn}/ϕ. In fact, the shift of T_c becomes less as either f_{AA} or f_{BB} is smaller. This conclusion is quite understandable if one consults Eq. (3) where the Potts part of the Hamiltonian takes its minimal and maximal as $f_{mn}=0.0$ and 1.0, respectively. Regarding the effect of domain size R on T_c, the simulated data show no identifiable shift of T_c unless $R<4$. As $R<4$, the DB's occupy most of the lattice and significant fluctuations of T_c shall be observed. It is then concluded that the hybrid model shows no essential difference in the static property from the pure Ising system unless R is very small. The simulation algorithm for the dynamic process can be the same as the conventional MC approach for the Ising system.

IV. DOMAIN BOUNDARY PRECIPITATION AND DOMAIN GROWTH

Our simulation starts from an initially random configuration of the Ising spins (A and B) in lattice. The Potts spins are distributed over the lattice via the same way as described in Sec. II. We choose $Q=24$, $C_0=0.10$, $L=256$, and occasionally 128. The parameters of interaction for two systems to be

TABLE II. The parameters of interaction for systems I and II.

System	ϕ_{AA}/kT_c	ϕ_{BB}/kT_c	T/T_c	J_{mn}/kT_c $(m,n=A,B)$	f_{AA}	f_{BB}	f_{AB}
I	0.00	0.00	4.40–0.22	1.20	1.0	0.0 or 1.0	$(f_{AA}+f_{BB})/2$
II	1.20	1.20	4.40–0.22	1.20	1.0	0.0 or 1.0	$(f_{AA}+f_{BB})/2$

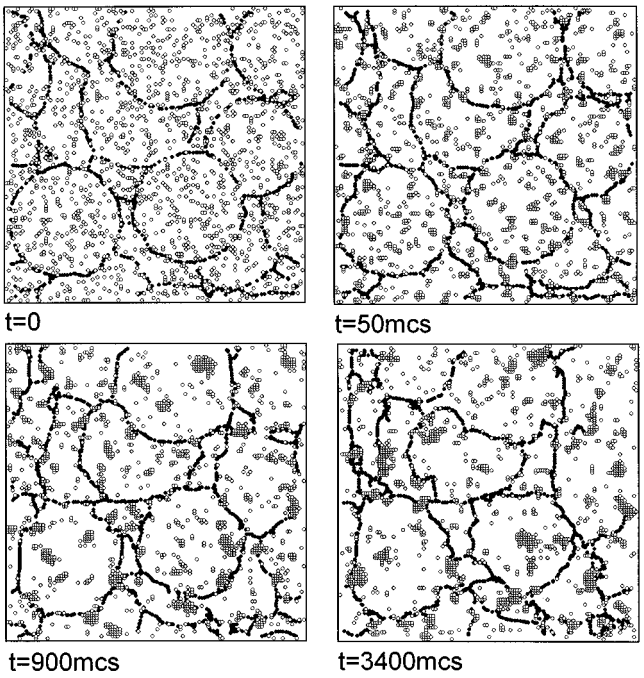

FIG. 3. Snapshot pictures of DB's configuration and solutes for system I at $T/T_c=0.8$ and $f_{BB}=1.0$. The time scales are inserted in the figures.

simulated are listed in Table II, where in system I domain growth is very slow and precipitation is dominant because $J_{mn} \gg \phi_{mm}$. This property allows one to choose much larger R than l_c, characteristic scale of the precipitated structure. For system II, the Ising events and the Potts ones are chosen with comparable probability (due to $J_{mn} \sim \phi_{mm}$) so that domain boundary migration becomes quite high. In this case, quite small initial domain size (e.g., $R=10$) is chosen, leaving enough space for the rapid domain growth. For both systems, strong segregation of solute B onto DB's is expected if $f_{BB}=0$, and no segregation is preferred if $f_{BB}=1.0$, because $f_{AA}=1.0$.

The MC algorithm and procedure of simulation were reported in our previous work,[29] and therefore will be no longer presented here. Note that the present algorithm is more efficient than the conventional Metropolis algorithm. For each system, at least four runs of simulation starting from different seeds of random number generation have been made and the average values of the simulated data are presented here. At $t=0$, the Ising spin for each site is chosen at random, whereas the domain size R ranges from 25–50 lattice units, and sometimes, 9–10 units for system II. We will first give a glance at the morphology of precipitates on DB's and then obtain a qualitative understanding of the influence of temperature. The domain growth features will also be described before a series of parameters are evaluated to characterize the precipitation at DB's and domain growth.

A. Precipitation and morphology of precipitates

For comparison, we first present in Fig. 3 the snapshot pictures of DB's configuration and solutes (B) at several times for system I at $T/T_c=0.8$ and $f_{BB}=1.0$, where no boundary precipitation is expected. In Fig. 4 are given the

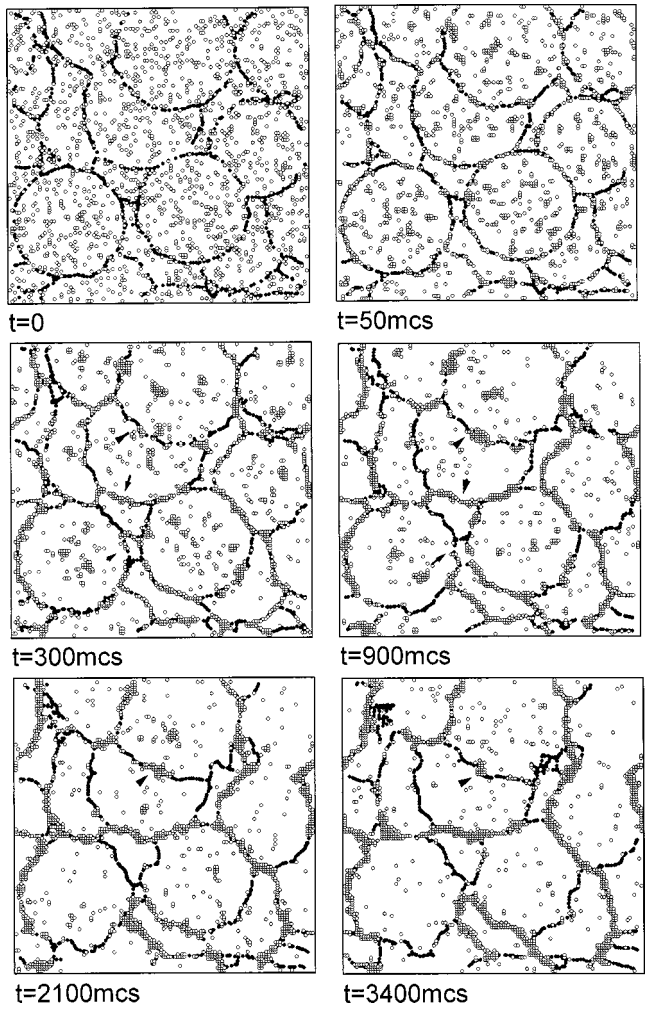

FIG. 4. Snapshot pictures of DB's configuration and solutes for system I at $T/T_c=0.8$ and $f_{BB}=0.0$. The time scales are inserted in the figures. The arrows indicate the boundaries that play as rapid channels for diffusion.

snapshot pictures at several times for the same system but $f_{BB}=0.0$. The solid circles represent DB's and the open circles represent solutes, leaving solvents A unlabeled.

From Fig. 3 it is clearly shown that in early stage [$t=5$ mcs (1 mcs represents a completed $L\times L$ circle)] the solutes begin to aggregate into small clusters, i.e., formation of small precipitates. Either growth or coarsening of the larger precipitates in compensation with shrinking of the smaller ones or coalescence of the smaller precipitates into larger ones is observed. The homogeneous phase precipitation[1] is shown, as predicted. Really, neither preference of precipitation on DB's nor shape anisotropy of the precipitates is identified. Nevertheless, it should be noted that here T is not far from T_c, and thus there exist a lot of monomers, dimers, trimers, and so on, in addition to the precipitates.

As $f_{BB}=0.0$, as shown in Fig. 4, very different kinetic phenomena are observed. Taking effect immediately from the quenching, the solutes are observed to aggregate along DB's, producing high boundary precipitation tendency. Many small precipitates inside domains are observed in early stage ($t=50$ mcs) in addition to those at DB's. The precipitates on DB's grow rapidly and interconnect with each other to form stripelike pattern along the local DB's. These stripes

become thicker and thicker across the DB's ($t=300 \sim 3400$ mcs). Most of the small precipitates initially inside domains shrink through monomer diffusion towards the DB's nearby them, although several of them occasionally coarsen through absorbing solutes surrounding them. At $t=3400$ mcs, it is rare to find precipitates inside the domains other than some individual solutes. Strong domain boundary precipitation is demonstrated in the present system.

There are several features worthy of mention for the boundary precipitation. First, the precipitates on DB's have stripelike shape. The shape of a local precipitate is completely determined by the local boundary shape. Second, the precipitate distribution on DB's is nonuniform. Some boundaries are completely occupied with precipitates whereas the others are less or nearly free of the solutes. This picture is easily understood because excess boundary energy is associated with the Potts-spin difference between adjunctive two domains. The boundaries with higher energy prefer the solute occupation. Third, it is recorded that DB's really play as a rapid channel for diffusion, although a quantitative characterization of such a sequence is still unavailable to the authors. As indicated by arrows in Fig. 4, the local boundaries attract the surrounding solutes and then transfer them to the neighboring boundaries where the higher energy is possessed and thus solutes become concentrated. Although the function of the local boundary as channel of diffusion depends more or less on the boundary property itself, those boundaries with moderate Potts-spin interaction play the best as the channels. In fact, in our simulation it is recorded that the average root-square shifting distance for each Ising spin at DB's is much larger than that for Ising spin far from DB's. In qualitative, one understands that the solutes to be trapped by the DB's of very high excess energy cannot shift away anymore as long as they are trapped. These DB's then become drains of solutes instead of channels of diffusion. The DB's of very low excess energy have little chance to collect solutes surrounding them. Nevertheless, those DB's of moderate excess energy can collect as many solutes around them as possible on one hand, on the other hand they transfer at a high probability the trapped solutes toward the neighboring DB's of high excess energy, resulting in rapid diffusion of solutes along these DB's.

B. Features of domain growth

In parallel to the boundary precipitation or aggregation, domain growth through boundary migration is also clearly identified in Fig. 4, although R is quite big. The domain growth looks to be isotropic and the domains are equiaxed because we impose a high value of Q ($Q=24$). The growth of larger domains in concert with shrinking of smaller ones is still observable in spite of slow boundary migration. Domain coalescence events are also occasionally identified. Four-domain junctions created through shrinking of the smaller domains become unstable and each finally splits into two trijunctions. The normal domain growth is displayed.[24–26]

However, a comparison of Fig. 4 with Fig. 3 shows serious pinning of DB's by the precipitates. When all boundaries in Fig. 3 change their locations from time to time, the highly solute-trapped boundaries shown in Fig. 4 do not change their locations too much. This effect becomes even more considerable as the boundary migration ability is high, to be shown later.

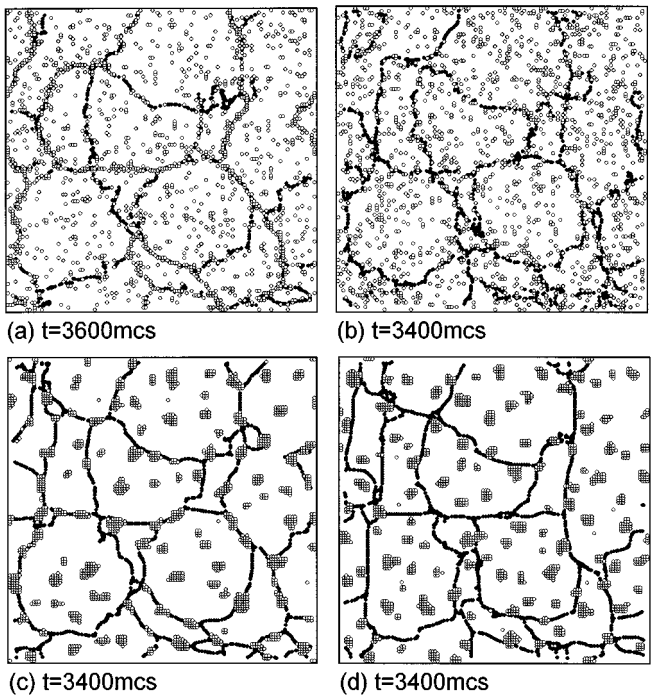

FIG. 5. Snapshot pictures of DB's configuration and solutes for system I at $T/T_c=2.5$ as $f_{BB}=0.0$ (a) and $f_{BB}=1.0$ (b), and $T/T_c=0.42$ as $f_{BB}=0.0$ (c) and $f_{BB}=1.0$ (d). The time scales are inserted in the figures.

C. Influence of temperature

We look at the effect of temperature on the morphology and kinetics of precipitates. In Figs. 5(a)–(d) two examples are given. In the top row are separately shown the configuration pictures for $T/T_c=2.4$ and $f_{BB}=0$ (a) and $f_{BB}=1.0$ (b). Note here that the system is in fact undersaturated since $T>T_c$. No aggregation of solutes is observed in Fig. 5(b). However, one identifies intensive solute segregation on DB's in Fig. 5(a), although the segregated clusters are dilute instead of compact. The thickness and length of the precipitates are much smaller than those shown in Fig. 4.

The more interesting point refers to the bottom row in Fig. 5, where the configurations at low T ($T/T_c=0.32$) are presented respectively for $f_{BB}=0$ (c) and $f_{BB}=1.0$ (d). Distinctive and large precipitates are formed at the early stage. If we would not have mapped the DB's, the lattice looks to be experiencing homogeneous precipitation at high supersaturation. Nevertheless, a careful identification reveals that many precipitates still prefer to stick on DB's as $f_{BB}=0.0$ [Fig. 5(c)]. The shape of precipitates on DB's is more or less equiaxed instead of stripelike pattern. However, the number density of the precipitate inside domains at $f_{BB}=0.0$ is lower than that at $f_{BB}=1.0$. This indicates that the boundary precipitation is no longer as remarkable as high T, although it is still preferred. It is thus demonstrated that the boundary precipitation features are very temperature dependent.

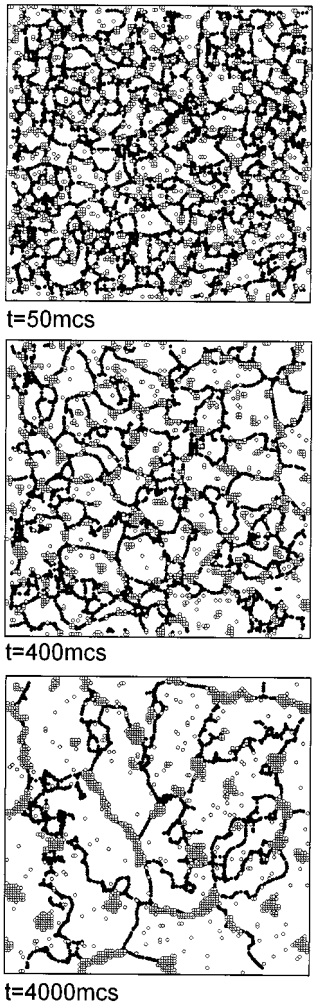

FIG. 6. Snapshot pictures of DB's configuration and solutes for system II at $T/T_c=0.8$ and $f_{BB}=0.0$. The time scales are inserted in the figures.

D. Features in the case of rapid boundary migration

Before evaluating quantitatively a series of parameters, let us look at what happens as DB's have high migration ability (i.e., system II). Figure 6 presents the snapshot pictures of DB's and solutes at several times for $T/T_c=0.8$ and $f_{BB}=0.0$. The boundary precipitation shows similar features as in system I, while here the domain growth becomes very fast. Nevertheless, system II has less remarkable boundary precipitation than system I. Due to the fast boundary migration, more precipitates are found inside domains because then can not catch up with the DB's at which they trapped earlier.

In addition, the pinning effect of DB's by the precipitates remains remarkable. The solute-concentrated boundaries hold unmoved with time. This effect, on the other hand, makes those solute-free boundaries highly rippled due to the fast motion. Regarding the effect of T, no significant difference is observed referred to systems II and I.

E. Occupation factor at DB's

In order to characterize the kinetics of the boundary precipitation and domain growth, we evaluate several parameters of the microstructure as a function of time and system parameters. First, we define an occupation factor of the solutes at DB's, Γ. It scales the number fraction of all domain boundary sites that are occupied with the solutes. This writes:

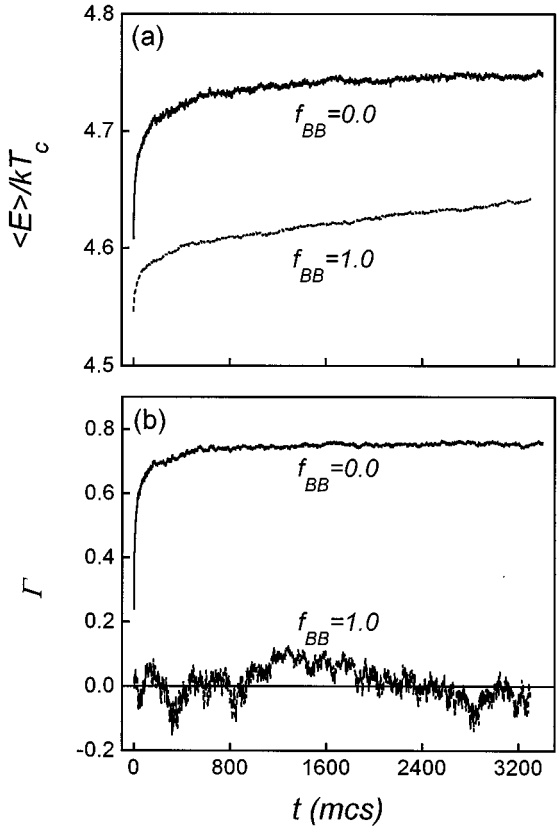

FIG. 7. $\langle E\rangle$ (a) and Γ (b) as a function of t for system I as $f_{BB}=1.0$ and $f_{BB}=0.0$; $T/T_c=0.80$.

$$\Gamma=(C_{DB}-C_0)/C_{DB}, \tag{7}$$

where C_{DB} represents the domain boundary sites occupied by the solutes normalized by all domain boundary sites. Obviously, $\Gamma=0$ if solutes have no preference to aggregate on DB's since $C_{\mathrm{DB}}\approx C_0$; $\Gamma=1-C_0$ if all domain boundary sites are occupied with solutes due to $C_{\mathrm{DB}}=1$; and $0<\Gamma<1-C_0$ otherwise.

In Fig. 7 are plotted against time the average energy of interaction per site, $\langle E\rangle=-H/L^2$, and Γ for $T/T_c=0.8$ at $f_{BB}=0.0$ (solid line) and 1.0 (dashed line). It is shown that for both cases $\langle E\rangle$ grows gradually and becomes slow at the late stage. Not only $\langle E\rangle$, but also the Potts interaction energy at DB's, can be fitted well with $\langle E\rangle\sim\exp(-\nu/t)$ where ν is a constant. That higher $\langle E\rangle$ at $f_{BB}=0.0$ than at $f_{BB}=1.0$ indicates that boundary precipitation rather than homogeneous precipitation is preferred thermodynamically. Γ fluctuates around $\Gamma=0$ as $f_{BB}=1.0$, but grows rapidly up to 0.70 in the early stage as $f_{BB}=0.0$. Afterwards it tends to be saturated at $\Gamma=0.75$. This tendency is consistent with the observation in Fig. 4. Note here that $\Gamma=0.75$ is already not far from the maximum $\Gamma=0.90$ (since $C_0=0.1$).

As $f_{BB}=0.0$, the simulated Γ at $t=1000$ mcs for different values of T/T_c are given in Fig. 8. Strong temperature de-

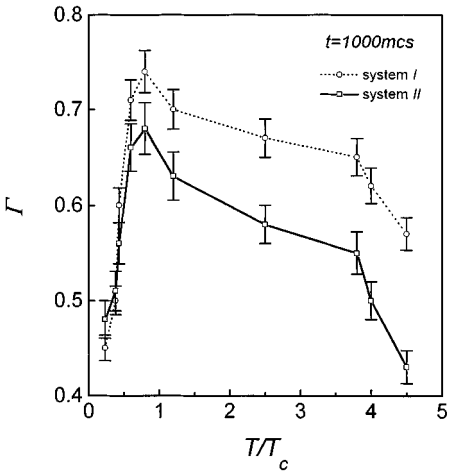

FIG. 8. Γ ($t=1000$ mcs) as a function of T/T_c for systems I and II as $f_{BB}=0.0$.

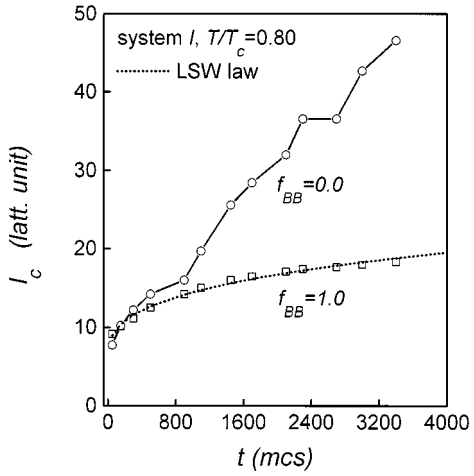

FIG. 9. l_c as a function of t for system I at $T/T_c=0.80$ as $f_{BB}=1.0$ and 0.0, respectively.

pendence of Γ is demonstrated. Interestingly, over the simulated range of temperature, Γ exhibits a single-peaked pattern. The peak position is located at $T/T_c\sim 0.8$ for both systems. On one side where $T>T_c$, solute aggregation on DB's is not serious, e.g., $\Gamma=0.57$ (I) and 0.43 (II) at $T/T_c=2.5$. On the other side, however, Γ is down to 0.45 at $T/T_c=0.32$. This corresponds to the case as shown in Fig. 5(c). The peak height of $\Gamma(T/T_c)$ for system II is a little lower than that for system I, indicating that a high mobility of DB's weakens the tendency of the boundary precipitation.

Figure 8 discloses a fact that strong domain boundary aggregation may only be achieved within a limited range of T/T_c. At either very low or very high temperature, weak solute aggregation on DB's and then a quasihomogeneous precipitation is expected.[17] We therefore argue that the maximal boundary precipitation tendency can be achieved only at a moderate supersaturation with T not far below T_c. In fact, this has been a well-known experimental phenomenon.[13]

To understand this phenomenon, we come to our model Eq. (1). As $T\gg T_c$, the thermal activation becomes very pronounced and any spin-aggregation event whose probability is determined by $\sim\exp(-\Delta H/kT)$, where ΔH is the energy difference after and before the event, will not be preferred very much due to large kT. Therefore precipitation either at DB's or inside domains is not favorable at high temperature. On the other hand, as $T\ll T_c$, i.e., at deep supersaturation, the solutes either nearby DB's or inside domains show very strong tendency of precipitation. They aggregate together very rapidly into stable precipitates. Note that only is considered the nearest-neighboring event (either Ising or Potts) in our model. Any solute desorption from existing precipitates is strongly unfavorable since $\Delta H/kT\gg 0$, unless the solute has its destination at DB's after one-step spin exchange. It is thus very hard for those solutes on the surface of existing precipitates that are at least two to three lattice units from any boundary site(s) to evaporate away. Therefore all precipitates inside domains remain quite stable against coarsening or segregation onto DB's.

F. Kinetics of precipitate growth and coarsening

We study the kinetics of growth and coarsening of the precipitates when the boundary precipitation is preferred. The spatial correlation function of the solutes in lattice can be defined as[3]

$$g(x,y,t)=\frac{1}{L\times L}\times\sum_{m,n}^{L\times L}(G(m,n,t)-C_0)\cdot(G(m+x,n+y,t)-C_0), \tag{8}$$

where $G(m,n,t)=0$ if site (m,n) is occupied by spin A, otherwise $G(m,n,t)=1$; x and y are the coordinates along the x axis and y axis, respectively. From Eq. (8), we can also define the axially oriented and radially averaged correlation functions:

$$g(x)=g(x,0,t),$$
$$g(y)=g(0,y,t), \tag{9}$$
$$g(r)=\frac{1}{M}\sum_{|\mathbf{r}|\le r<|\mathbf{r}|+i}g(x,y,t),\quad \mathbf{r}=\mathbf{i}x+\mathbf{j}y,$$

where M is the number of $g(x,y,t)$ which satisfies $|r|\le r<|r|+1$ overall the lattice sites and $g(r)$ represent the radial average of $g(x,y,t)$. Considering the fact that no considerable anisotropy of the precipitate distribution appears, we only present our analysis of $g(r)$ below.

$g(r)$ oscillates around the r axis. The wavelength l_c scales the average size of the precipitates and it is comparable to the interprecipitate spacing. Therefore time evolution of l_c characterizes growth and coarsening of the precipitates. In Fig. 9 are plotted $l_c(t)$ for system I at both $f_{BB}=1.0$ and 0.0. As $f_{BB}=0.0$ l_c achieves rapid growth over the simulated period, referring to the case of $f_{BB}=1.0$. Especially at $T/T_c=0.8$, l_c for $f_{BB}=0.0$ is three times that for $f_{BB}=1.0$ as $t=3400$ mcs. Furthermore, different kinetic behaviors of l_c for $f_{BB}=0.0$ and 1.0 is identified. For $f_{BB}=1.0$, the growth shows continuously decelerating, whereas a roughly linear growth of l_c is observed in case of $f_{BB}=0.0$.

Regarding the effect of temperature on the kinetics, one presents the simulated data of l_c at different T/T_c as $f_{BB}=0.0$ in Figs. 10(a) and (b) for systems I and II, respectively. Note here once more that there is no precipitate observed at

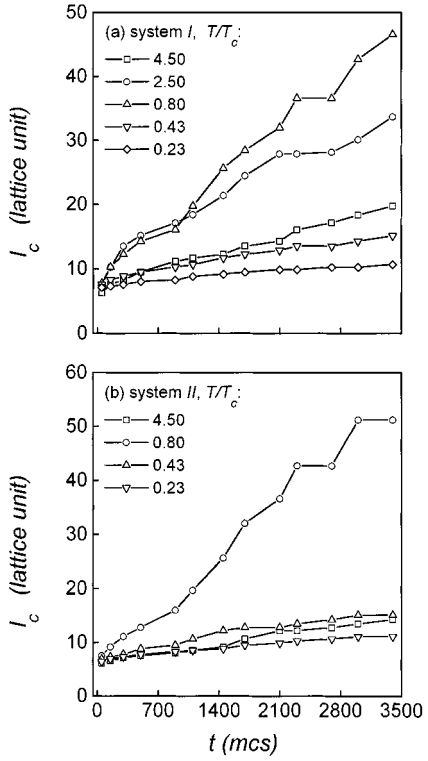

FIG. 10. l_c as a function of t at various T/T_c as $f_{BB}=0.0$, for system I (a) and system II (b), respectively.

$T/T_c>1$ as $f_{BB}=0$, however, domain boundary segregation yields. $g(r)$ still produces an oscillation. The data of $l_c(t)$ thus evaluated are presented in Fig. 10 for comparison. It is seen strong dependence of $l_c(t)$ on T/T_c. At similar time scale, l_c shows growth with decreasing of T at $T>T_c$, then decays with decreasing of T at $T<T_c$. The peak of $l_c(T)$ is again roughly located at $T/T_c=0.8$. It is easily understood that this dependence is attributed to the same reason that determines $\Gamma(T)$, as just discussed in the previous section. Let us see again $l(t)$ at various T/T_c for both systems I and II, a roughly linear relation is established at higher T/T_c, whereas a negative deviation from the linearity is observed as T/T_c is quite low. This deviation is more remarkable in system II than in system I. As is well known, the LSW law is usually used to characterize the kinetics of precipitate coarsening in alloys, the present simulation provides us an opportunity to check this law in case of domain boundary segregation. More details are presented in Sec. III H.

G. Kinetics of domain growth

In this section the kinetics of domain growth is emphasized. The aim is to check the normal linear law for domain growth as domain boundary segregation features are considered. We apply the random sampling technique to evaluate the domain area distribution $f(A,t)$ and define the average domain area $\langle A\rangle$ as[23]

$$\langle A\rangle=\sum_i A\cdot f(A,t)\Big/\sum_i f(A,t). \tag{10}$$

Although the sampling per lattice fluctuates due to limited size ($L=256$), an averaging processing on more than ten samplings gives quite good data. The evaluated data of $\langle A\rangle$ as a function of t for system I at $T/T_c=0.8$ are presented in Fig. 11. $\langle A\rangle$ at $f_{BB}=0.0$ is smaller than that at $f_{BB}=1.0$. This difference becomes even more remarkable toward the late stage. It allows one to argue that domain growth is hindered by precipitates at DB's. For system II, similar results are revealed. Furthermore, $\langle A\rangle$ exhibits a roughly linear dependence of t at $f_{BB}=1.0$, whereas this dependence becomes much weaker at $f_{BB}=0.0$. This fact predicts that the kinetics of domain growth deviates from the normal kinetic law as the domain boundary precipitation is favored.

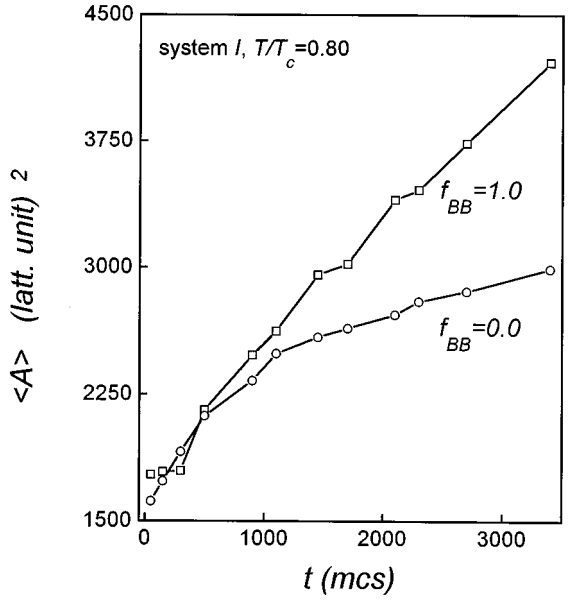

FIG. 11. $\langle A\rangle$ as a function of t for system I at $T/T_c=0.80$ as $f_{BB}=1.0$ and 0.0, respectively.

This time dependency of $\langle A\rangle$ for systems I and II at $f_{BB}=0.0$ under different T/T_c are given in Fig. 12. At a similar time scale, $\langle A\rangle$ for system II is much higher than that for system I. The reason is quite obvious. It is also observed that $\langle A\rangle$ decreases as T/T_c decreases, because the mobility of the precipitates is lowered at low T. This effect pins DB's from moving and then hinders growth of the domains.

H. Broken LSW law and growth exponent

As we mentioned above, the precipitate coarsening shows quite different kinetic behavior, depending on whether strong domain boundary segregation is preferred or not. Thus there is a need to recheck the applicability of the LSW law and related growth exponent. As is well known, coarsening of multiprecipitated microstructure controlled uniquely by solute diffusion follows the LSW law, owing to the potential difference in precipitate/matrix interface between two neighboring precipitates of different size.[38,39] Suppose that total volume of precipitates is constant and low, and the size distribution of precipitates is $p(l,t)$; we can write following continuum equation to be satisfied during the coarsening:[8,9]

$$\frac{\partial p}{\partial t}+\frac{\partial}{\partial l}\left[p\frac{\partial l}{\partial t}\right]=0. \tag{11a}$$

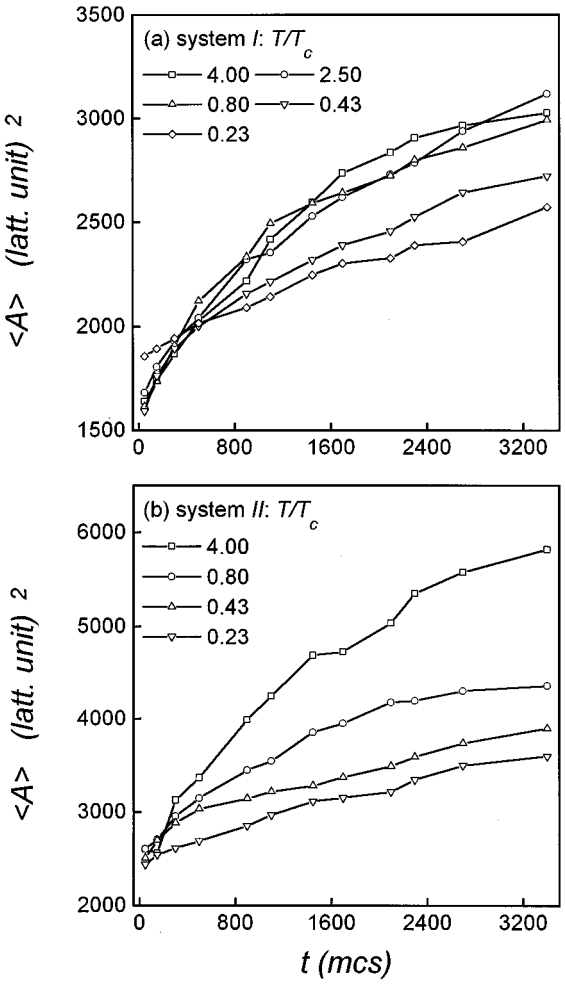

FIG. 12. $\langle A\rangle$ as a function of t at various T/T_c as $f_{BB}=0.0$, for system I (a) and system II (b), respectively.

Toward the late stage of coarsening, distribution $p(l,t)$ remains stationary although its position shifts toward the large size side. This means that there exists an average precipitate size l_c satisfying the following equation:[38]

$$\frac{dl_c}{dt}=\rho_1\frac{D\cdot\sigma_{AB}}{T}\cdot\frac{1}{l_c^2}, \tag{11b}$$

where ρ_l is a positive constant, D is the solute diffusion coefficient, and σ_{AB} is the interface energy between the precipitate and matrix (i.e., B cluster and A matrix). Equation (11b) yields

$$l_c(t)^3-l_c(t=0)^3=(3\rho_1\cdot D\cdot\sigma_{AB}/T)\cdot t=K\cdot t, \tag{12a}$$

where K is a positive constant. Equation (12a) is the well-known LSW law. As $l_c(t=0)=0$, Eq. (12a) yields the well-known power law with growth exponent $\gamma=\frac{1}{3}$.

$$l_c=\sqrt[3]{\rho_1\cdot D\cdot\sigma_{AB}/T}\cdot t^{\gamma}\propto t^{\gamma}. \tag{12b}$$

In our hybrid model, the precipitate coarsening at $f_{BB}=1.0$ is nearly pure-diffusion controlled. The evaluated $l_c(t)$ indeed follows the $\frac{1}{3}$ power law, as shown in Fig. 9. As $f_{BB}=0.0$, considerable domain boundary aggregation is observed, indicating existence of a strong attractive potential between precipitates and DB's. Equation (11b) should include this additional attractive term. A reasonable approach to the problem starts from adding a new term to the right-hand side of Eq. (11b):

$$\frac{dl_c}{dt}=\rho_1\frac{D\cdot\sigma_{AB}}{T\cdot l_c^2}+\rho_2\frac{D\cdot\Omega_{\mathrm{DB}}}{T\cdot R}, \tag{13}$$

where ρ_2 is a positive constant on the same order of magnitude as ρ_1 ($\rho_1\sim\rho_2$), Ω_{DB} is the potential difference between two precipitate inside domains and at DB's, respectively, separated by $\sim R$. This term reflects the attractive interaction between DB's and precipitates inside domains. Ω_{DB}/R should have the same unit as σ_{AB}. As the zero-order approximation, for example, σ_{AB} and Ω_{DB} may easily be written as[2]

$$\sigma_{AB}\sim-\frac{1}{4}\phi_{AB}\sim kT_c/4,$$

$$\Omega_{\mathrm{DB}}/R\sim 4J_{BB}(1-f_{BB})\sim 5kT_c(1-f_{BB}).$$

Clearly, one has $\Omega_{\mathrm{DB}}/R\gg\sigma_{AB}$ as f_{BB} is zero. On the other hand, domain growth is a slow sequence with respect to precipitation, i.e., $dl_c/dt\gg dR/dt$. Therefore R can be approximately viewed as a constant in Eq. (13). The solution to Eq. (13) reads if $l_c(t=0)=0$ and constants $\rho_1\sim\rho_2\sim 1$:

$$l_c=\sqrt{\frac{\sigma_{AB}R}{\Omega_{\mathrm{DB}}}}tg^{-1}\left(l_c\sqrt{\frac{\Omega_{\mathrm{DB}}}{\sigma_{AB}R}}\right)+\frac{D\cdot\Omega_{\mathrm{DB}}}{T\cdot R}t. \tag{14a}$$

As mentioned above, if $\Omega_{\mathrm{DB}}/R\gg\sigma_{AB}$ is satisfied and l_c is not very small, one has as the zero-order approximation

$$l_c\sim\frac{D\cdot\Omega_{\mathrm{DB}}}{T\cdot R}t. \tag{14b}$$

This equation may not be a quantitatively acceptable expression of the coarsening phenomenon, but shows the influence of DB's in a qualitative way. The growth exponent $\gamma=1$ for the precipitate coarsening is established in case of serious domain boundary segregation, well consistent with our simulated data shown in Figs. 9 and 10. Furthermore, it is seen from Eq. (14) that l_c grows at a lower rate as T is lower because term D/T is a decaying function of T, and a large domain size corresponds to a slow growth of l_c. As R is quite large, Eq. (14b) may be no longer a good approximation of Eq. (14a). A negative deviation of Eq. (14a) from the linearity is expected. We then have $1/3<\gamma<1$. All of these predictions are well confirmed with our data shown in Figs. 10(a) and (b) (see our analysis in Sec. III F).

For a better understanding of growth exponent γ, one uses Eq. (12b) to fit the simulated data and the evaluated γ as a function of T/T_c is plotted in Fig. 13(a). It is seen that for both systems $\gamma=0.33\pm0.04$ at $f_{BB}=1.0$, independent of T/T_c. Very good consistency of the simulated data with the LSW law is indicated. However, at $f_{BB}=0.0$, γ no longer keeps unchanged but shows a value much larger than the LSW exponent 0.33. It increases first and then decreases with decreasing of T/T_c. The maximal, very close to 1, is reached at $T/T_c=0.8$. Nevertheless, note here that at low temperature ($T/T_c<0.4$) γ reapproaches the LSW exponent.

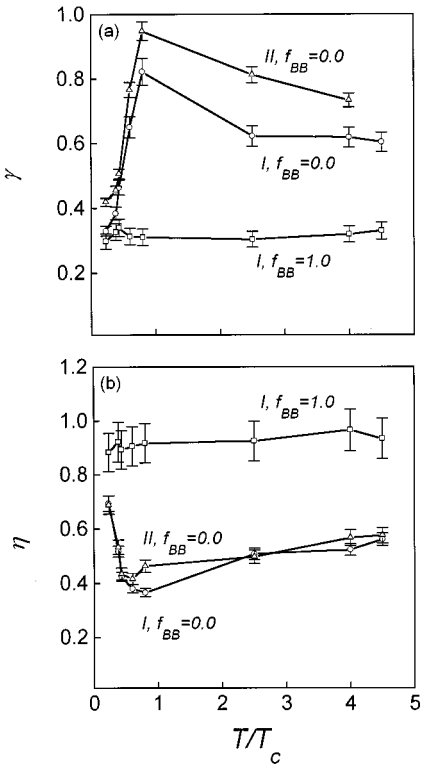

FIG. 13. Growth exponent γ for precipitate coarsening (a) and the exponent η for the domain growth at various T/T_c as $f_{BB}=1.0$ and 0.0, for systems I and II.

The reason is that the second term on the right-hand side of Eq. (14a) decays very rapidly with decreasing of T. The first term on the right-hand side of Eq. (14a) becomes relatively important at low T, thus resulting in γ recovering back to the LSW exponent. In fact, to date most of the evidences from experiments and simulations refer to the cases of deep supersaturation, so that the LSW law has achieved widespread support. We therefore conclude that the coarsening of the precipitate depends on the domain boundary segregation behavior and the LSW law becomes no longer applicable for the case of favored boundary segregation.

I. Broken linear law and exponent of domain growth

Now we come to check the linear law for domain growth sequence. The domain growth is solely driven by the excess energy associated with DB's. For normal domain growth, it is assumed that the domain size follows a monodispersed distribution, therefore the property of average domain area $\langle A\rangle \sim R^2$ uniquely characterizes the behavior of domain growth. The kinetics can be described by[24–26]

$$\frac{dR}{dt}=\varphi\left(\frac{D_{\mathrm{DB}}}{T}\right)\frac{\Sigma_{\mathrm{DB}}}{R}, \tag{15a}$$

where φ is a positive constant, D_{DB} is the coefficient scaling the mobility of DB's, and Σ_{DB} is the domain boundary energy. The latter can be roughly treated as a time-independent quantity. One thus has the well-known linear law

$$\langle A\rangle=\langle A\rangle_0+2\varphi(D_{\mathrm{DB}}/T)\Sigma_{\mathrm{DB}}\cdot t, \tag{15b}$$

where $\langle A\rangle_0$ is $\langle A\rangle$ at $t=0$. A growth exponent $\eta=1$ is then defined and well confirmed by real and computer experiments. Our simulated data of $\langle A\rangle$ as a function of t, as shown in Fig. 11 at $f_{BB}=1.0$ where normal domain growth is expected, support this linear law. However, Eq. (15b) is no longer true when domain boundary segregation is favored ($f_{BB}\ll 1$), because Σ_{DB} here is no longer time independent but decays with sinking of solutes onto DB's. Because our simulation reveals that H_P in Eq. (1) decreases exponentially with time, simply, one can rewrite Eq. (15a) as

$$\frac{dR}{dt}=\varphi\left(\frac{D_{\mathrm{DB}}}{T}\right)\frac{\Sigma_{\mathrm{DB}}[1-\exp(-\tau/t)]}{R} \tag{16a}$$

with τ the characteristic time. Apart from the early stage of domain growth ($t\gg\tau$), one obtains an approximate solution to Eq. (16a):

$$\langle A\rangle=\langle A\rangle_0+2\varphi(D_{\mathrm{DB}}/T)\Sigma_{\mathrm{DB}}\cdot\tau\ln(t). \tag{16b}$$

Therefore a negative deviation of $\langle A\rangle$ from the normal linear law is predicted, confirmed with our simulated data shown in Figs. 11 and 12 at $f_{BB}=0.0$. Regarding the effect of T, one understands that (D_{DB}/T) decays rapidly with T so that $\langle A\rangle$ shows slower growth at lower T, no matter what f_{BB} takes. The data evaluated at various T/T_c at $f_{BB}=0.0$ for both systems I and II qualitatively support Eq. (16), as shown in Fig. 12.

Nevertheless, people are used to applying a power law:

$$\langle A\rangle=\langle A\rangle_0+b\cdot t^{\eta},\quad b>0 \tag{17}$$

with growth exponent η to fit the domain growth data. In fact, Eq. (16b) may not be a quantitative acceptable law due to a series of approximations made. We prefer to apply Eq. (17) to evaluate the value of η, rather than using Eq. (16b). The results are shown in Fig. 13(b). At $f_{BB}=1.0$, the simulated data for both systems fluctuate around $\eta=0.95$, independent of T. The normal kinetics of domain growth is demonstrated. When the boundary segregation is favored, the data are much lower than the normal value $\eta=1.0$. The difference reaches the maximum at $T/T_c=0.6$–0.42, where the simulated value $\eta=0.40\pm0.05$. As expected, the simulated η at very low T ($T/T_c=0.23$) recovers up to 0.73, not far from the normal value. Therefore we are allowed to conclude that the normal law of domain growth is broken and no longer applicable as long as the domain boundary segregation is strongly favored.

J. Scaling of precipitated microstructure and domain size

Finally, we come to check the scaling state of both the precipitated microstructure and the domain growth. The scaling of the precipitated microstructure reflects a stationary state achieved in lattice with respect to the unique characteristic length l_c. In the diffusion-limited aggregation, all of the correlation properties of the microstructure should hold stationary after rescaled with l_c, leaving l_c to grow according to some power law.[1,3] However, in case of the strong boundary segregation, l_c is not only determined by the diffusion but also dependent of DB's, so that the scaling state may no longer be reached.

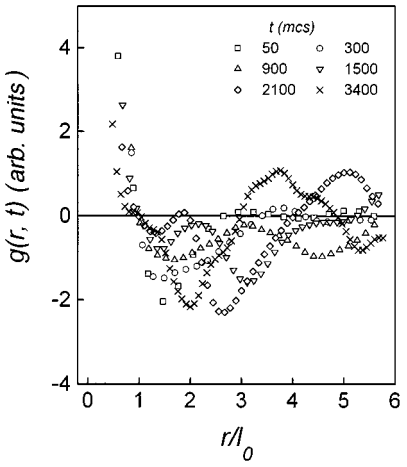

FIG. 14. Invalid scaling processing of correlation function $g(r,t)$ at various times as $T/T_c=0.80$ and $f_{BB}=1.0$ for system I.

In Fig. 14 are shown $g(r)$ at several times for system *I* as $T/T_c=0.8$ and $f_{BB}=0.0$. The curves are rescaled by the first crossing point l_0 at which $g(l_0)=0$, so they may fall onto the same curve if the scaling state would have been reached. Anyway, these data points look to be still far from falling onto one specific curve. This allows us to conclude that no scaling relation is satisfied with the microstructure, at least until the longest time we reached, $t=3400$ mcs (this time scale equals to 10^4 mcs in the conventional Metropolis algorithm). It provides us the first evidence that the scaling law for homogeneous second phase precipitation may no longer be applicable when domain boundary segregation is strongly favored. It should be mentioned that as evaluating the data at low *T*, we do observe that the system approaches the scaling state but never reaches it at the longest time scale reached.

On the other hand, it was revealed earlier that the domain shape and topological relations at DB's do not change remarkably during domain growth. Although the kinetic exponent shows serious deviation from the normal value, it is surprising that the scaling for domain growth still holds. The data of scaling processing are presented in Figs. 15(a) and (b) for system II where domain growth is developed over large spatial scale. It is clearly shown that for each case all data after $t\geqslant 900$ mcs fall onto one specific curve $F(A/\langle A\rangle)$ within the statistical uncertainty, demonstrating the scaling property of domain growth even when domain boundary segregation and precipitation are strongly favored. The same conclusion works for system I too.

Nevertheless, what should be pointed out here is that the scaling for domain growth may still require rechecking at a much large spatial scale. The lattice size employed in present work may be large enough for simulation of precipitated microstructure, but not large enough for domain growth simulation. Furthermore, the domain size that can be described by this hybrid model is small and the number of domains involved for statistics in the late stage is not enough. In fact, if one replots $F(A/\langle A\rangle)$ just over a small $A/\langle A\rangle$ range, says from 0–2.5, the curves at various times still show some differences to each other. Therefore the conclusion on the domain growth scaling may not be convincing before a much larger scale simulation is carried out (for example, $L>1024$). We just show that the present data look

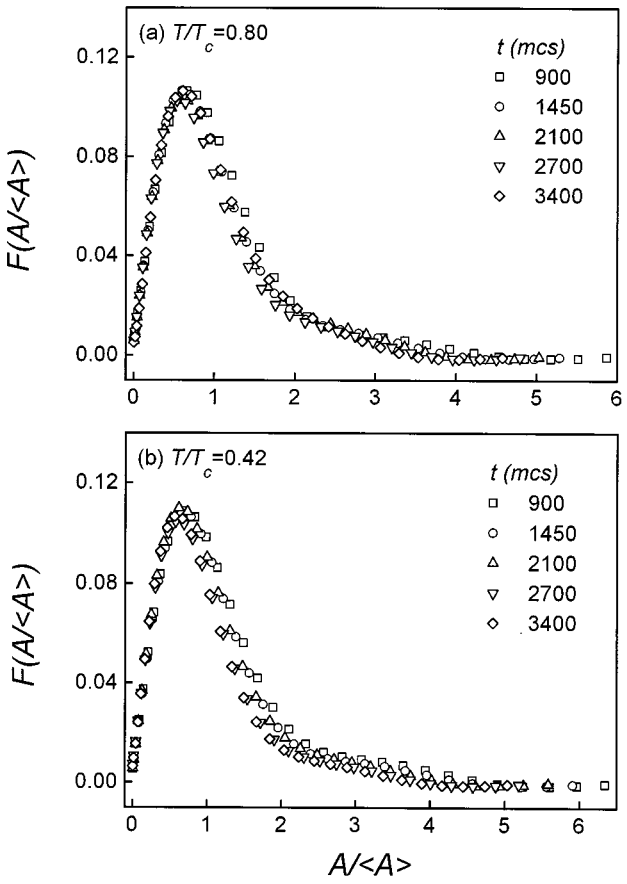

FIG. 15. Scaling of the domain area distributions at various times as $f_{BB}=0.0$ for system II.

supportive of the conclusion that the scaling holds for the domain growth even in the case of strong boundary segregation.

K. Remarks

A number of interesting features associated with second phase precipitation and domain growth are basically attributed to the coupling between the Ising model and Potts model. What should be pointed out here is that the Ising spin states are conserved whereas the Potts-spin states are not. The conservation of the Ising spins limits coarsening of the precipitated microstructure so that a power law of $\frac{1}{3}$ is achieved. The growth exponent for domain growth becomes $\frac{1}{2}$ (taking the linear dimension $R\sim t^{\eta}$, we have $\eta=\frac{1}{2}$) due to the nonconservation of the Potts spins. A coupling of the two types of spin states produces a balancing point between $\frac{1}{3}$ and $\frac{1}{2}$.

The reason that favors the scaling property of domain growth is the high *Q* states chosen for constructing the Potts lattice, which results in a roughly isotropic boundary configuration even after a long period of growth.

V. SOME RELEVANCES TO REAL ALLOY SYSTEMS

We have presented in detail our simulated results and revealed a series of interesting phenomena in the binary systems where both domain boundary precipitation and domain growth proceed in parallel. Especially, we have demon-

strated that the LSW law and scaling property of the phase precipitation are broken when the boundary segregation is preferred. For domain growth, an abnormal kinetics has been revealed although the scaling property may still hold. Just viewing from the kinetics of either phase precipitation or domain growth, the precipitate coarsening is accelerated whiles the domain growth is decelerated. Nevertheless, real alloy systems may not perform as simply as we have shown above. Many kinetic and structural features associated with precipitation and boundary segregation in polycrystalline materials cannot be imaged by our approach Eq. (1). For example, real alloys decompose via the spin-vacancy exchange mechanism instead of spin-spin exchange. In a number of cases, the precipitate phase is structurally ordered compound. Formation of the new second phase accompanies the generation of long-range stress field. It is impossible to approach all of these features and very hard to deal with them in a preliminary sense. However, considering the fact that our hybrid model is intrinsically of short range, it is still helpful to give a preliminary discussion on effect of vacancies and kinetics of second-ordered compound in the framework of Eq. (1). A detailed simulation of them is left for future work.

A. Spin-vacancy exchange mechanism

An alloy contains a number of vacancies, third species V besides species A and B. The spin-vacancy exchange is a realistic mechanism for species diffusion. An acceptable assumption is that there is no interaction between vacancies and species, whether the Ising-type or Potts-type. Therefore Eq. (1) still remains applicable for the A-B-V system.[34] However, the MC algorithm and procedure for the Ising sequence have to be modified, whereas the algorithm and procedure for domain growth remain unchanged because the Potts event does not need spin exchange. For the Ising sequence, a site is chosen only if it is occupied by a vacancy or it has neighboring vacancy. If a vacant site is chosen, it is permitted to do exchange with any of its four neighbors. The site must do exchange with its vacant neighbor if it is taken by A or B. A spin-vacancy exchanging event is approved by the same probability criterion.

This modified approach was used to simulate homogeneous second phase precipitation in single-crystalline solution.[34] Basically, there is no difference in the microstructural and dynamic features between the spin-spin exchange mechanism and the spin-vacancy exchange one. The vacancies have no tendency of aggregation but simply distribute at random in lattice. However, in our hybrid model the vacancies inside domains will be attracted toward DB's to consume part of the excess energy there. This sequence is especially preferred at $f_{BB}=1.0$ rather than $f_{BB}=0.0$. It is easily understood that they will not self-aggregate but just distribute randomly along DB's.

What should be pointed out here is that $\phi_{AA}=\phi_{BB}=0$ is assumed in our model. It means that the like-spin pairs have no interaction, the same as the species-vacancy pairs. This choice avoids any precipitation tendency of vacancies themselves, but is less relevant for real alloys because vacancy segregation at the interfacial layer of A phase and B phase and DB's as well is observed in real alloys.[40,41] It is therefore necessary to take positive ϕ_{AA} and ϕ_{BB} and keep ϕ unchanged for our simulation. In this case, vacancy aggregation at the A/B phase interface was confirmed.[42] For the present hybrid model, vacancies may aggregate at A/B phase interface or DB's, depending on a competition of H_I and H_P via the aggregation.

B. Precipitation of ordered compound

Equation (1) may also be used to describe precipitation of ordered A-B compound in the multidomained lattice. Strictly speaking, a correct description of precipitation of stoichiometric ordered AB compound requires inclusion of the next-nearest-neighboring Ising interaction between species A and B.[43] Therefore Eq. (1) has to be modified for such a description. Suppose that the second phase is an $ABAB$-type ordered compound, there will appear a number of small $ABAB$ ordering domains (OD's) in lattice until the Ising-spin balance is reached, following by coarsening of the larger OD's in concert with shrinking of the smaller ones. Note here that growth of the OD's may not require long-range diffusion of species, the kinetics of the ordering-domain growth obeys $\frac{1}{2}$ power law[44] instead of the LSW law for pure second phase coarsening.

Regarding the interaction of DB's and OD's, at $f_{BB}=1.0$ one may not be able to observe any interaction between them. However, when $f_{BB}<1.0$ or 0.0, segregation of the solutes at DB's may be observable. In such a case, the Ising-spin conservation introduces repulsive force between DB's and OD's. This implies that the formed OD's have a tendency of keeping away from the DB's nearby. Domain boundary segregation will hinder coarsening of the OD's although the OD's far from DB's may coarsen via the normal mechanisms. This problem remains of special interest and is worthy of detailed study.

VI. CONCLUSION

In conclusion, we have studied by means of MC method the static properties of the Ising-Potts hybrid model proposed earlier, referring to phase separation and domain growth in binary alloys. It has been demonstrated that a coupling of the Ising lattice with the Potts spins shifts the Ising critical point toward a lower temperature. This effect is, however, quite weak, especially in the case of the strong domain boundary segregation expected. The domain boundary precipitation and domain growth as parallel processes in binary alloys are simulated in detail. We have revealed significant boundary precipitating phenomena at a temperature just below the critical point for the alloys where the solutes prefer onto domain boundaries. At either high or low temperature, the tendency of boundary precipitation is considerably weakened. The strong temperature dependence of the morphology and size of the second phase, including those precipitating at domain boundaries, is established. Typically stripelike boundary precipitates are observed. Due to the favored boundary precipitation, the coarsening of the second phase is remarkably accelerated. No matter what the migration ability of domain boundaries, the domain growth is seriously pinned by the boundary precipitates, although the domain pattern

and dynamic property of the boundary migration remain normal. Both the Lifshitz-Slyozov-Wagner law for the precipitate coarsening and the linear law for the domain growth are found to break due to the boundary precipitation phenomenon. When the scaling state for the precipitated microstructure can never be reached, the scaling property of the domain growth may still hold in spite of further confirmation required. We have also discussed the possibility of applying the present model to some problems relevant to real alloy systems, indicating a number of interesting effects to be explored.

ACKNOWLEDGMENTS

The authors would like to thank Professor C. K. Ong for encouragement of this work. The simulation was carried out at Nanjing University of China under the support of the National Natural Science Foundation of China through the Special Program.

*Author to whom correspondence should be addressed. Electronic address: liu-jm@imre.org.sg

[1] For a review, refer to R. Wagner and R. Kampmann, in *Materials Science and Technology: A Comprehensive Treatment*, edited by P. Haasen (VCH Publishers Inc., New York, 1991), Vol. 5, p. 213.
[2] P. Haasen, *Physikalische Metallkunde* (Springer-Verlag, Berlin, 1984).
[3] K. Binder, in *Materials Science and Technology: A Comprehensive Treatment* (Ref. 1), Vol. 5, p. 405.
[4] J. D. Gunton, M. San Miguel, and P. S. Sahni, in *Phase Transitions and Critical Phenomena*, edited by C. Domb and J. L. Lebowitz (Academic, New York, 1983), Vol. 5, p. 202.
[5] K. Binder and D. Stauffer, Phys. Rev. Lett. **33**, 1066 (1974).
[6] J. Marro, J. L. Lebowitz, and M. H. Kalos, Phys. Rev. Lett. **43**, 282 (1979).
[7] J. S. Langer, M. Baron, and H. D. Miller, Phys. Rev. A **11**, 1417 (1975).
[8] I. M. Lifshitz and V. V. Slyozov, J. Phys. Chem. Solids **19**, 35 (1961).
[9] C. Wagner, Z. Electrochem. **65**, 243 (1961).
[10] E. T. Gawlinski, J. D. Gunton, and J. Vinal, Phys. Rev. B **39**, 7266 (1989).
[11] T. M. Rogers, K. P. Elder, and D. C. Desai, Phys. Rev. B **37**, 9638 (1988).
[12] D. A. Huse, Phys. Rev. B **34**, 7845 (1986).
[13] G. R. Purdy, in *Materials Science and Technology: A Comprehensive Treatment* (Ref. 1), Vol. 5, p. 305.
[14] A. G. Khachaturyan, *Theory of Structural Transformations in Solids* (Wiley, New York, 1983).
[15] P. Fratzl and O. Penrose, Acta Mater. **44**, 3227 (1996).
[16] J. Singh, G. Jerman, R. Poorman, B. N. Bhat, and A. K. Kuruvilla, J. Mater. Sci. **32**, 3891 (1997).
[17] Y. Saito, Mater. Sci. Eng., A **223**, 125 (1997).
[18] K. S. Chan, L. H. Chen, and T. S. Liu, Mater. Trans., JIM **38**, 420 (1997).
[19] F. F. Gong, H. M. Shen, and Y. N. Wang, Appl. Phys. Lett. **69**, 2656 (1996).
[20] M. Thuvander, K. Stiller, D. Blavette, and A. Menand, Appl. Surf. Sci. **94/95**, 343 (1996).
[21] J. H. Kim and W. K. Choo, J. Phys. IV **5**, 329 (1995).
[22] V. E. Fradkov and D. Udler, Adv. Phys. **43**, 739 (1994).
[23] J. Stavans, Rep. Prog. Phys. **56**, 733 (1993).
[24] W. W. Mullins, J. Appl. Phys. **59**, 1341 (1986).
[25] M. P. Anderson, D. J. Srolovitz, G. S. Grest, and P. S. Sahni, Acta Metall. **32**, 783 (1984).
[26] G. S. Grest, M. P. Anderson, and D. J. Srolovitz, Phys. Rev. B **38**, 4752 (1988).
[27] D. N. Fan, L. Q. Chen, and S. P. Chen, Mater. Sci. Eng., A **238**, 78 (1997).
[28] D. N. Fan and L. Q. Chen, Acta Mater. **45**, 3297 (1997).
[29] J. M. Liu, Phys. Rev. B **58**, 633 (1998).
[30] K. Kawasaki, in *Phase Transitions and Critical Phenomena* (Ref. 4), Vol. 2, p. 443.
[31] N. Metropolis, A. W. Rosenbluth, A. H. Teller, and E. Teller, J. Chem. Phys. **21**, 1987 (1953).
[32] F. Y. Wu, Rev. Mod. Phys. **54**, 235 (1982).
[33] C. P. Flynn, *Point Defects and Diffusion* (Clarendon, Oxford, 1972).
[34] K. Yaldram and K. Binder, Acta Metall. Mater. **39**, 707 (1991).
[35] K. W. Kehr, K. Binder, and S. M. Reulein, Phys. Rev. B **39**, 4891 (1989).
[36] H. Furukawa, Adv. Phys. **34**, 703 (1985).
[37] K. Binder and D. W. Heermann, *Monte-Carlo Simulation in Statistical Physics: An Introduction* (Springer-Verlag, Berlin, 1988).
[38] J. M. Martin and R. D. Doherty, *Stability of Microstructure in Metallic Systems* (Cambridge University Press, Cambridge, England, 1976), p. 163.
[39] K. Tsumuray and Y. Miyata, Acta Metall. **31**, 437 (1983).
[40] M. Militzer, W. P. Sun, and J. J. Jonas, Acta Metall. Mater. **42**, 133 (1994).
[41] S. H. Zhang, X. L. He, and T. Ko, J. Mater. Sci. **29**, 2663 (1994).
[42] J. M. Liu, Scr. Mater. **37**, 535 (1997).
[43] L. Q. Chen and A. G. Khachaturyan, Acta Metall. Mater. **39**, 2533 (1991).
[44] T. Ohta, D. Jasnow, and K. Kawasaki, Phys. Rev. Lett. **49**, 1223 (1982).